Quantum signal transmission through a single-qubit chain

Ya. S. Greenberg[1], C. Merrigan[2], A. Tayebi[3,4], and V. Zelevinsky[4,5]
[1] *Department of Physics and Techniques, Novosibirsk State Technical University, Novosibirsk 630092, Russia*
[2] *William Jewell College, Liberty, Missouri 64068, USA*
[3] *College of Engineering, Michigan State University, East Lansing, Michigan 48824, USA*
[4] *Department of Physics and Astronomy, Michigan State University, East Lansing, Michigan 48824, USA and*
[5] *National Superconducting Cyclotron Laboratory, Michigan State University, East Lansing, Michigan 48824, USA*
(Dated: February 12, 2013)

A system of a two-level atom of an impurity (qubit) inserted into a periodic chain coupled to the continuum is studied with the use of the effective non-Hermitian Hamiltonian. Exact solutions are derived for the quasistationary eigenstates, their complex energies, and transport properties. Due to the presence of the qubit, two long-lived states corresponding to the ground and excited states of the qubit emerge outside the Bloch energy band. These states remain essentially localized at the qubit even in the limit of sufficiently strong coupling between the chain and the environment when the super-radiant states are formed. The transmission through the chain is studied as a function of the continuum coupling strength and the chain-qubit coupling; the perfect resonance transmission takes place through isolated resonances at weak and strong continuum coupling, while the transmission is lowered in the intermediate regime.

PACS numbers:

I. INTRODUCTION

Open quantum systems are currently in the center of attention of physicists in different subfields. The main driving force in this direction is evidently the quest for the new progress of quantum informatics. Another area with significant recent achievements related to openness of a quantum system is nuclear physics, where the understanding of structure and reactions of loosely bound nuclei far from stability requires the correct unified treatment of bound states and continuum. Cold atoms in traps and optical lattices can give rise to new effects of coupling, entanglement and transfer of information. Solid-state micro- and nano-devices, including Josephson junctions and spintronics, are probably the most developed arrangements of this type.

From a general point of view, in all cases we have to deal with a mesoscopic system of interacting constituents that serves as a guide for the transmission of a quantum signal. The system can have intrinsic degrees of freedom which can be excited and deexcited by the signal. The coupling to the external world is realized through a certain amount of channels characterized by the asymptotic quantum numbers of emitted particles or quanta and the final state of the system. Each channel has an energy threshold where it becomes open and connects to the environment. In the absence of decoherence through external noise or a heat bath, the transmission at given energy is described by the unitary scattering matrix in the space of channels open at this energy. All these features are common for numerous loosely bound or marginally stable mesoscopic systems determining their main observable properties.

A convenient mathematical formalism for description of such systems is given by the effective non-Hermitian Hamiltonian; this method based on the Feshbach projection formalism[1,2] is formally exact but very flexible and can be adjusted to many specific situations; see the recent review article[3] that covers applications to the continuum shell model in nuclear physics and, in less detail, to the quantum signal transmission through simple periodic and disordered chains. To stress the breadth of possible problems solved in this approach we can mention recent applications to arrays of antennas[4] and studies of light harvesting bacteria in the same framework[5].

One bright phenomenon emerging in the situation with a relatively strong continuum coupling in the case when the number of open channels is relatively small compared to the number of involved intrinsic states is the so-called *super-radiance*. Being an analog of super-radiance in quantum optics[6,7], this term stands for the formation in the system of a collective superposition of the intrinsic states coherently coupled to the same decay channel. The number of possible states of this type is equal to the number of open channels.

The simplest transmission system fully studied with the aid of the effective non-Hermitian Hamiltonian is an open periodic chain with hopping between adjacent cells[8–13]. It was shown[14] that, after appropriate identification of parameters, this system is physically equivalent to a realistic sequence of quantum barriers. The transmission was studied at weak continuum coupling (a system of narrow individual resonances) and in the limit of strong coupling when the resonances overlap and the main role is played by the physics of super-radiance (collectivization through continuum). The limit of overlapping resonances is usually described, in the tradition borrowed from nuclear physics, in terms of Ericson fluctuations[15]; it was shown that this theory should be corrected in a number of aspects, including the correct account for the unitarity that is the main source of super-radiance. The behavior of an ideal periodic

system was juxtaposed to the case of disorder, where the super-radiance still survives, and it is possible to establish the connection to the Anderson model, degree of chaos inside the system and universal conductance fluctuations. The consideration was also extended to grids with two- and three-dimensional geometry; an especially interesting case is presented by the *star graph*[16] where a number of open channels intersect at a common central point. At this point an analog of a bound state (evanescent wave) with a long lifetime exists that can serve for accumulation of quantum information.

Thanks to the development of nanotechnology, the preparation of low-dimensional assemblies of nanoparticles becomes a routine experimental task[17]. This renews the attention to the study of quantum properties of relatively simple low-dimensional mesoscopic systems which reveal a rich physical behavior. In this context, the exactly solvable models as tight-binding one- or two-dimensional chains coupled to adatoms or impurities are of special interest[18–21].

In what follows we consider a similar system with a two-level atom of an impurity (qubit) inserted into an open periodic chain. The model is simple enough to allow for the exact solution; at the same time the model turns out to be rich enough to demonstrate interesting physics of the signal transmission. An analytical consideration is supplemented by the detailed numerical study for the chain with eleven sites.

The paper is organized as follows. In Sec. 2 we consider a *closed* chain of $2N$ identical cells with the nearest neighbor hopping interaction. Two arms of the chain are connected through the central cell occupied by a two-level atom (qubit). We find the energy spectrum of the system that consists of a normal band of delocalized Bloch standing waves and two additional states outside the band corresponding to the excited and the ground states of the qubit. We study the evolution of the energy spectrum as a function of the chain-qubit coupling strength.

Sec. 3 describes the energy spectrum of the *open* system coupled to the continuum through its edge states. The former stationary states acquire decay widths that change as a function of the coupling constants. The decay widths of the qubit states are small compared to those of the Bloch waves. The qubit states remain essentially localized at the qubit even when the coupling of the chain to the continuum becomes sufficiently strong to allow for the formation of super-radiant states.

In Sec. 4 we study the transmission through the chain as a function of the coupling parameters. In both limits of the edge continuum coupling being weak and strong compared to the coupling between the qubit levels, the resonances are well isolated all having narrow decay widths and perfect transmission at resonance energies. When both couplings are of comparable strength, the resonances are overlapped and the transmission is below the perfect level. The results are summarized in the Conclusion.

II. CLOSED CHAIN

We consider a linear chain of $2N$ identical cells numbered as $n = -N, -(N-1), ..., -1$ and $n = 1, ..., N-1, N$, while the central cell, $n = 0$, is occupied by a qubit, a two-level atom with states $|0\rangle$ and $|e\rangle$, excitation energy $\epsilon_e - \epsilon_0 = \Delta$, and matrix element λ of the qubit excitation. The energy ϵ_0 is the level position in all cells; for simplicity we put the lower level of the isolated qubit at the same position. Introducing the hopping (tunneling) matrix element v between the neighboring cells, we come to the Hamiltonian of the closed chain:

$$H_{nn} = \epsilon_0, \quad H_{n,n+1} = H_{n+1,n} = v, \quad n = -N, ..., 0, ..., N; \tag{1}$$

$$H_{ee} = \Delta, \quad H_{0e} = H_{0e} = \lambda, \tag{2}$$

where all matrix elements can be considered as real.

Before introducing the coupling to the outside world, we briefly characterize the solution for the closed chain. A general stationary state $|E\rangle$ with energy E can be presented as a superposition

$$|E\rangle = \sum_{n=-N}^{N} c_n(E)|n\rangle + b(E)|e\rangle. \tag{3}$$

The boundary conditions for the chain closed at the edges are $c_{-N-1} = c_{N+1} = 0$. The coefficients of the superposition (3) satisfy the obvious equations:

$$(E - \epsilon_0)c_n - v(c_{n-1} + c_{n+1}) = 0, \quad n \neq 0, \tag{4}$$

$$(E - \epsilon_0)c_0 - v(c_{-1} + c_{+1}) = \lambda b, \tag{5}$$

$$(E-\Delta)b=\lambda c_0. \tag{6}$$

Eqs. (5) and (6) can be treated as boundary conditions for the two chains (left and right) implying that

$$c_0(E)=\frac{v(E-\Delta)}{(E-\epsilon_0)(E-\Delta)-\lambda^2}\,(c_{-1}+c_1). \tag{7}$$

Following the same procedure as for a single chain[8], see also Appendix in Ref.[12], we find that the solutions on both sides of the qubit have the form

$$c_n=\begin{cases} A\xi_+^n+B\xi_-^n,\ n<0;\\ A'\xi_+^n+B'\xi_-^n,\ n>0. \end{cases} \tag{8}$$

The amplitudes $\xi_\pm$ are given by

$$\xi_\pm=\frac{1}{2v}\left[E-\epsilon_0\pm\sqrt{(E-\epsilon_0)^2-4v^2}\right], \tag{9}$$

and $\xi_+\xi_-=1$. The edge conditions determine

$$B=-A\left(\frac{\xi_-}{\xi_+}\right)^{N+1},\quad B'=-A'\left(\frac{\xi_+}{\xi_-}\right)^{N+1}. \tag{10}$$

The central point determines two classes of solutions. The *antisymmetric* states, $c_1+c_{-1}=0$, have $c_0=0$, so that these wave functions are decoupled from the excited qubit that lives on the excited level $E=\Delta$ (in this situation the qubit can be excited or deexcited only by an additional external coupling). Because of $c_0=0$ and interaction only between the neighboring cells, the two sides of the chain are also decoupled from each other so that such modes do not take part in the transport through the whole chain. The spectrum E_q of the antisymmetric states is determined by the roots of $\xi_-^{2N+2}=1$ that can be parameterized by the even-number quantized quasimomentum q, or by the phase φ_q,

$$E_q=2v\cos\varphi_q,\quad \varphi_q=\frac{\pi q}{2N+2},\quad q\ \text{even}, \tag{11}$$

and the local amplitudes (8) of the wave functions are

$$c_n(q)=i^q\sqrt{\frac{1}{N+1}}\,\sin(n\varphi_q). \tag{12}$$

The energies (11) are inside the Bloch band $(-2v,+2v)$.

The *symmetric* solutions, $c_1=c_{-1}$, involve the qubit into dynamics and the corresponding roots are determined by

$$\xi_+^{2N+2}=\frac{\lambda^2+(E-\Delta)\sqrt{(E-\epsilon_0)^2-4v^2}}{\lambda^2-(E-\Delta)\sqrt{(E-\epsilon_0)^2-4v^2}}. \tag{13}$$

To derive this relation, it is convenient to use eq. (4) and connect the amplitude c_1, or c_{-1}, to the central amplitude c_0,

$$c_1=-c_0\,\frac{\xi_+^N-\xi_-^N}{\xi_+^{N+1}-\xi_-^{N+1}}. \tag{14}$$

With the qubit disconnected, $\lambda\to 0$, we have the missing in eq. (11) q-odd part of the band spectrum with the amplitudes (12) where $\sin(n\varphi_q)$ is changed to $\cos(n\varphi_q)$. When the qubit is connected to the chain, the upper level is outside the band, $E>2v$; the lower level also leaves the band at a finite value of λ when $E<-2v$. The full spectrum of twelve energy levels for $N=5$ is shown as a function of λ in Fig. 1. The upper state starts at $E=\Delta$ and grows approximately linearly with λ. At small λ, this is the state with the excited qubit and only weak admixtures of intrinsic sites.

With increasing λ, the symmetric and antisymmetric states inside the band become degenerate, while the excited (upper) wave function is spread almost equally over two states of the qubit. The orthogonal combination of the excited and ground state of the qubit gives the lower state (at sufficiently large values of λ). In this limit the picture effectively is of Rabi oscillations between the qubit levels with only a small probability of hopping along the chain. The chain then is almost decoupled from the qubit. This evolution of the two wave functions is illustrated by Fig. 2.

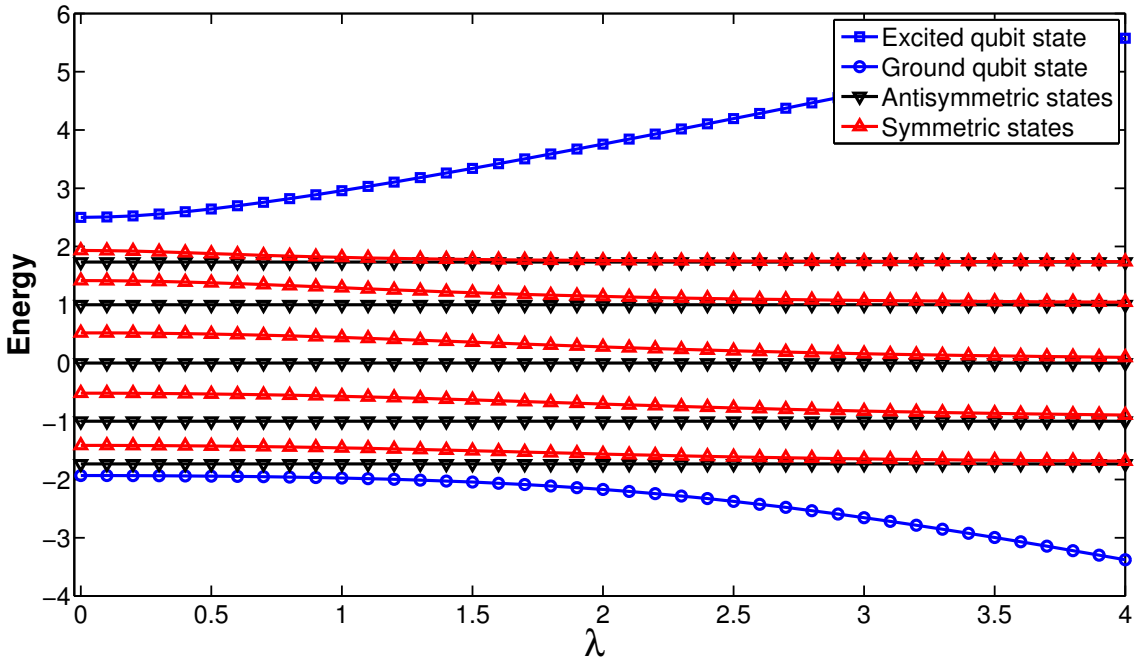

FIG. 1: (Color online). Energy levels for a system of the closed chain of eleven sites and the excited qubit state in the middle as a function of the qubit coupling strength λ; the hopping amplitude is set to $v = 1$, and the excitation energy of the qubit $\Delta = 2.5$.

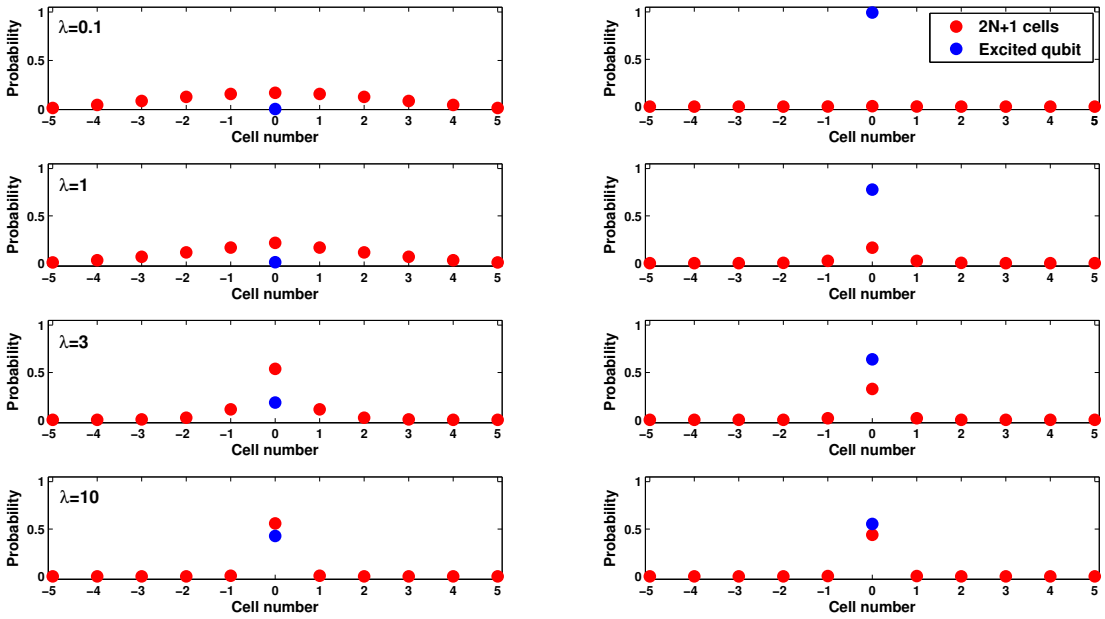

FIG. 2: (Color online). Squared components of the lower (left column) and upper (right column) of the wave functions as a function of the qubit excitation strength λ, for a chain $N = 5$ and $v = 1$.

III. OPEN CHAIN

Now we assume that the edge states are coupled to the outside world by ideal leads and the situation becomes identical with what can be described by the effective non-Hermitian Hamiltonian,

$$\mathcal{H} = H - \frac{i}{2}W, \tag{15}$$

acting only in the intrinsic space of the closed system. Here the anti-Hermitian part W is factorized[3] having the matrix elements W_{12} between the intrinsic states $|1\rangle$ and $|2\rangle$ in the form of the product of partial amplitudes A_1^c and A_2^c which generate the interaction between intrinsic states through an open decay channel c,

$$W_{12} = \sum_{c;\,\mathrm{open}} A_1^c A_2^c. \tag{16}$$

It is important that here the superscript c runs only over open channels (*on-shell* interaction). In general the amplitudes A_1^c are energy-dependent vanishing at the threshold energy for a given channel, and their near-threshold behavior determines the non-exponential decay curve in the long-time limit. In many cases this dependence can be ignored, which we assume in this work as well.

In the case of a linear chain we allow only left and right decays through the edge states (it would be also interesting to study the decoherence through the coupling with many "random" weak channels connected to the intrinsic sites). The factorized nature of the operator W (dictated essentially by requirements of unitarity of the scattering matrix in the channel space, see for example[22]), shows that this operator has only few non-zero eigenvalues their number being equal to the number of open channels. The corresponding eigenstates are obviously just the edge states directly coupled to the continuum. Therefore it is sufficient in our scheme to introduce two complex energies, ϵ_R and ϵ_L for the states at the edges, where $\epsilon_{L,R} = \epsilon_0 - (i/2)\gamma_{L,R}$. Such an open system without a qubit was analyzed in Refs.[8,10,12,14]. In this approach the states directly coupled to the continuum play the role of doorways[23], and the remaining states can get their widths (finite lifetimes) only through their coupling to the doorways.

The typical situation for the chain without a qubit is evolving as a function of parameters $\gamma_{L,R}$ compared to the level spacing D in the closed system. At weak coupling, every intrinsic state becomes a resonance with a small decay width determined by the overlap of the Bloch state with the edges; the final width distribution has, for $\gamma_L = \gamma_R$, a maximum in the center of the band. In the limit of strong continuum coupling, we have a super-radiant situation when the central state accumulates almost the entire width while the remaining states become very long-lived (trapped). In the case of $\gamma_L \neq \gamma_R$ there occur two super-radiant transitions[12] with the maximum of the signal transmission in between. In the site representation, the super-radiant states with energies in the center of the band are located at the edges. This picture survives also the possible presence of disorder in the intrinsic wells[10].

The results for the chain with the qubit are illustrated by the series of graphs, where the chain consists of 5+1+5=11 cells with the qubit in the middle, altogether 12 intrinsic states. Here we diagonalize the effective Hamiltonian in the *doorway representation*: the continuum coupling occurs only at the edges which serve as doorways, and the matrix elements of the anti-Hermitian part of the effective Hamiltonian (15), which couples the states $|q\rangle$ with the outside world, are given in the band representation by

$$W_{qq'} = \gamma_L c_{-N}(q) c_{-N}(q') + \gamma_R c_N(q) c_N(q'). \tag{17}$$

Fig. 3 shows the evolution (as a function of λ) of the resonance energies for the case of weak continuum coupling, $\gamma_L = \gamma_R = 0.1$ (the scale is fixed by the band width, $v = 1$). At small λ, we have the parabolic distribution of widths with the maximum at the center of the band, as known from previous studies[8,10], and the decoupled excited qubit state above the band with zero width. As λ increases, the symmetric and antisymmetric states merge becoming effectively decoupled from the qubit. The excited qubit state and emerging outside the band the ground qubit state are still almost stationary (*Rabi regime*). They are moving along the real energy axis being repelled by the band.

The situation changes when we come to the strong continuum coupling, Fig. 4. Here we again follow the evolution as a function of λ but at $\gamma = 20$. At small $\lambda = 0.1$, the two coinciding super-radiant states are formed in the center of the band (here we keep $\gamma_L = \gamma_R$), and the remaining ten states are trapped, effectively returning to the non-overlap regime (the left lower plot shows, at a much smaller width scale, the parabolic width distribution). With increase of λ, the super-radiant states survive, while the qubit states again are repelled by the band along the real energy axis having still very small widths.

It is instructive to take a look of the width evolution as a function of the continuum coupling strength γ. The typical process is presented by Fig. 5, where the trajectories of all twelve complex poles in the lower half of the complex plane are shown. In the limit of very weak continuum coupling, part (*a*) of this figure, the width distribution

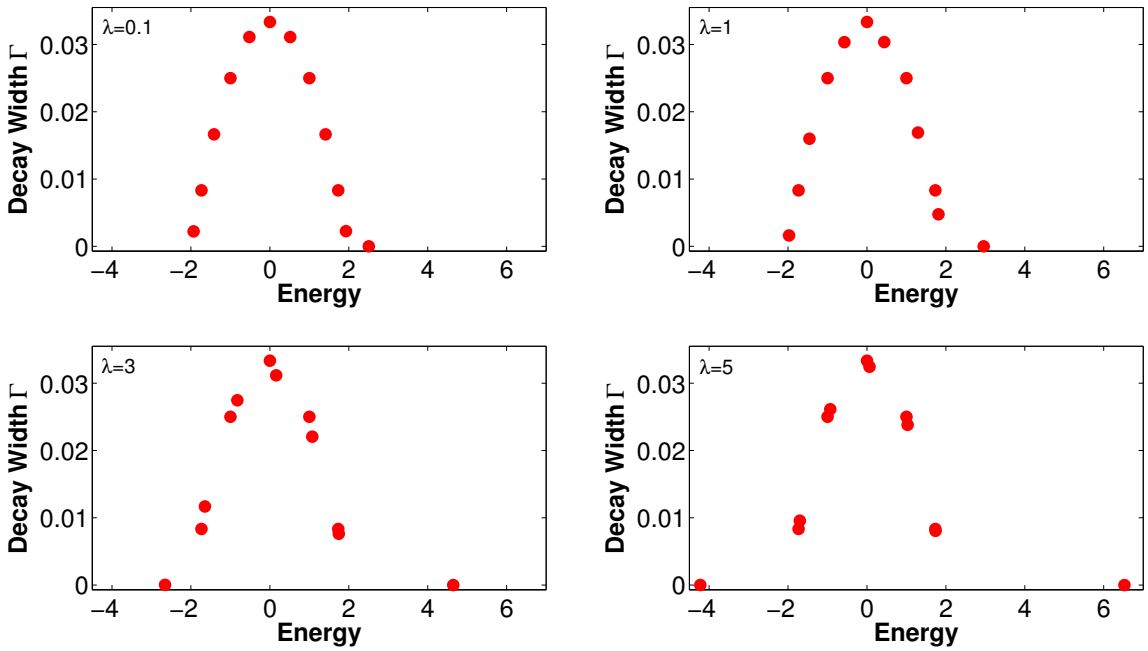

FIG. 3: (Color online). Resonance complex energies (eigenvalues of the effective Hamiltonian for weak continuum coupling, $\gamma = 0.1$) evolve as a function of the qubit excitation strength λ. Two qubit states are effectively decoupled from the chain and move along the real energy axis.

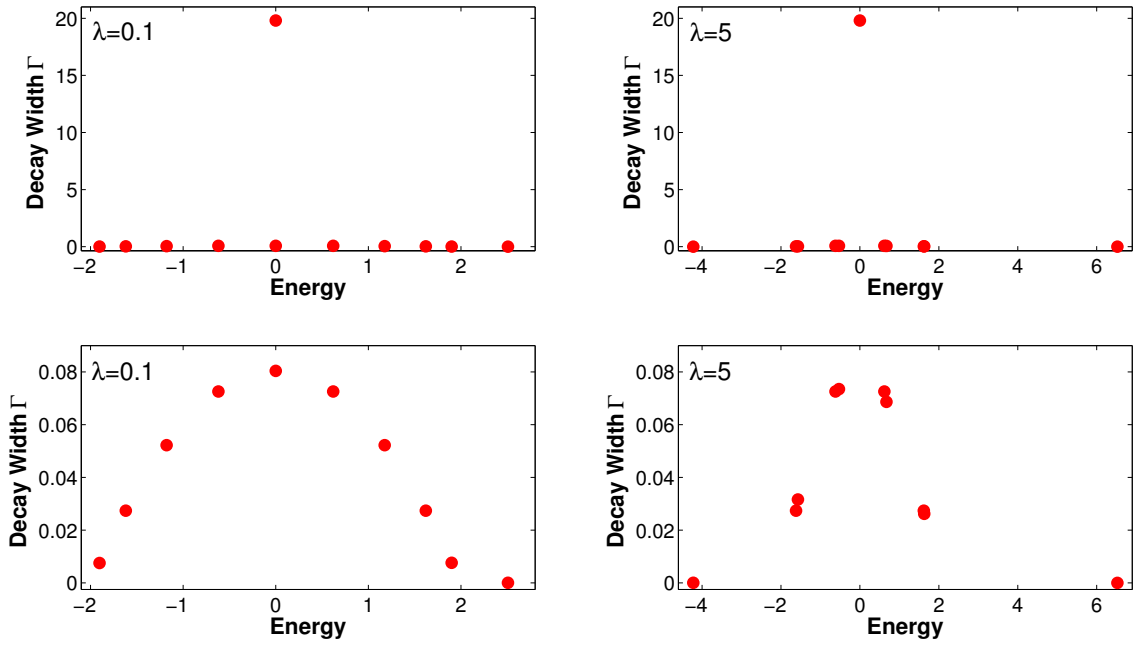

FIG. 4: (Color online). Resonance complex energies (eigenvalues of the effective Hamiltonian for strong continuum coupling, $\gamma = 20$) show segregation of two super-radiant states in the middle of the band from ten trapped states which include the strongly localized states of the qubit.

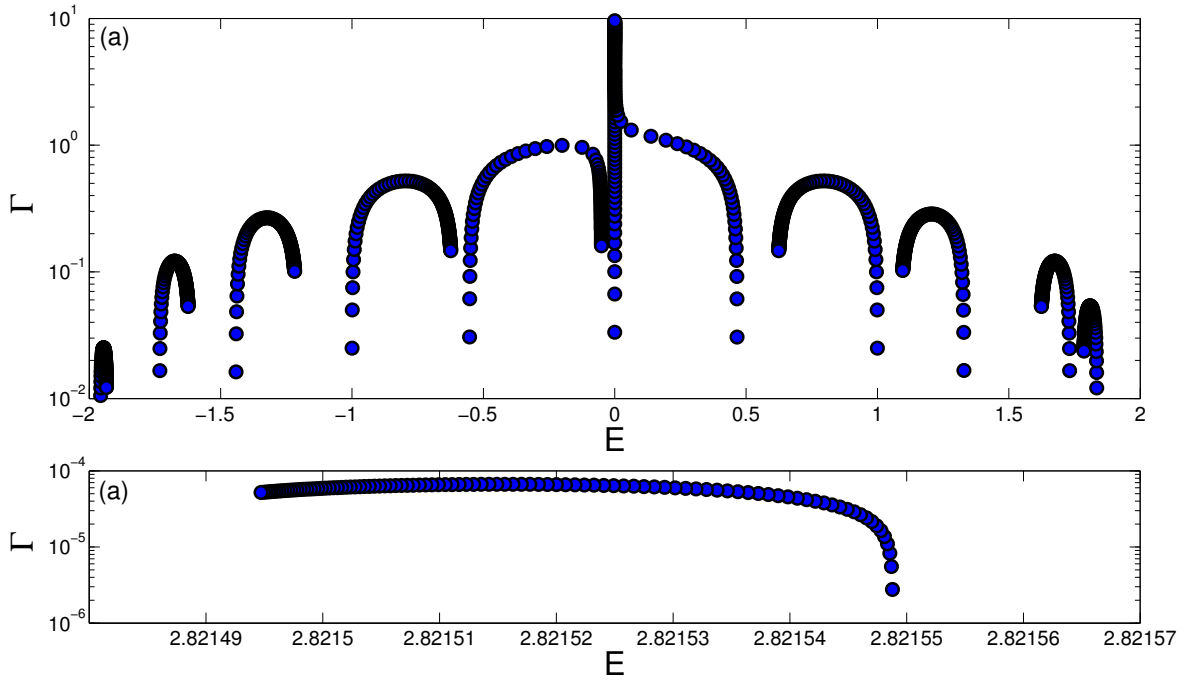

FIG. 5: (Color online). Complex-plane trajectories of eigenstates of the effective Hamiltonian; the parameter values are $v = 1,\ \lambda = 0.8,\ \Delta = 2.5$. Panel ($a$) shows the behavior of 12 states in the chain while panel (b) singles out the state genetically connected to the excited qubit state located outside the band.

is parabolic, being proportional, as a function of real energy, to the group velocity of the band states. It is transformed with increase of γ. All widths, except for the super-radiant states in the center of the energy band, turn back after reaching their maximum values. Their corresponding trajectories are almost symmetric with respect to their maxima which is typical for the phenomenon of super-radiance in a space of fixed dimension. Indeed, after the segregation of the super-radiant state(s), the remaining trapped states are essentially in the same situation as they were in the beginning of the process; this symmetry for the finite dimension of intrinsic space is a characteristic feature[12] that appears also in the statistical distribution of neutron widths for thermal-energy neutron resonances[24]. Part (b) of the figure selects, on a detailed energy scale, the complex-plane evolution of the excited qubit state that becomes extremely long-lived. The details of interference between neighboring resonances were also discussed repeatedly in the context of the electron conduction in nano-scale systems, see for example[25].

It was noticed long ago[26] that, in the description of an open system with the aid of the effective Hamiltonian, the Hermitian and non-Hermitian parts of the interaction act in the opposite way. The real (Hermitian) perturbation repels the levels but, through the mixing mechanism, attracts the width of unstable states. Contrary to that, the imaginary (non-Hermitian) interaction through the continuum repels the widths (the road to superradiance and trapping) but attracts real energies of resonances. This attraction is seen in Fig. 6 for a larger value of λ: as the continuum coupling γ increases along the road to super-radiance, the real energies of the poles move to the middle of the band, where the super-radiant states are located.

Finally, the limit of very strong coupling between the qubit levels is shown in Fig. 7 where $\lambda = 8$. As antisymmetric and symmetric roots merge with increasing continuum coupling γ, we see, panel (a), the evolution of pairs of states (ten of them inside the band including the super-radiant ones). The time arrow of this evolution is again in the direction of attraction for the real energies of resonances. The qubit states, the ground state, (b), and the excited state, (c), are essentially decoupled. They do not shift and only gradually increase their (still small) decay widths as γ increases.

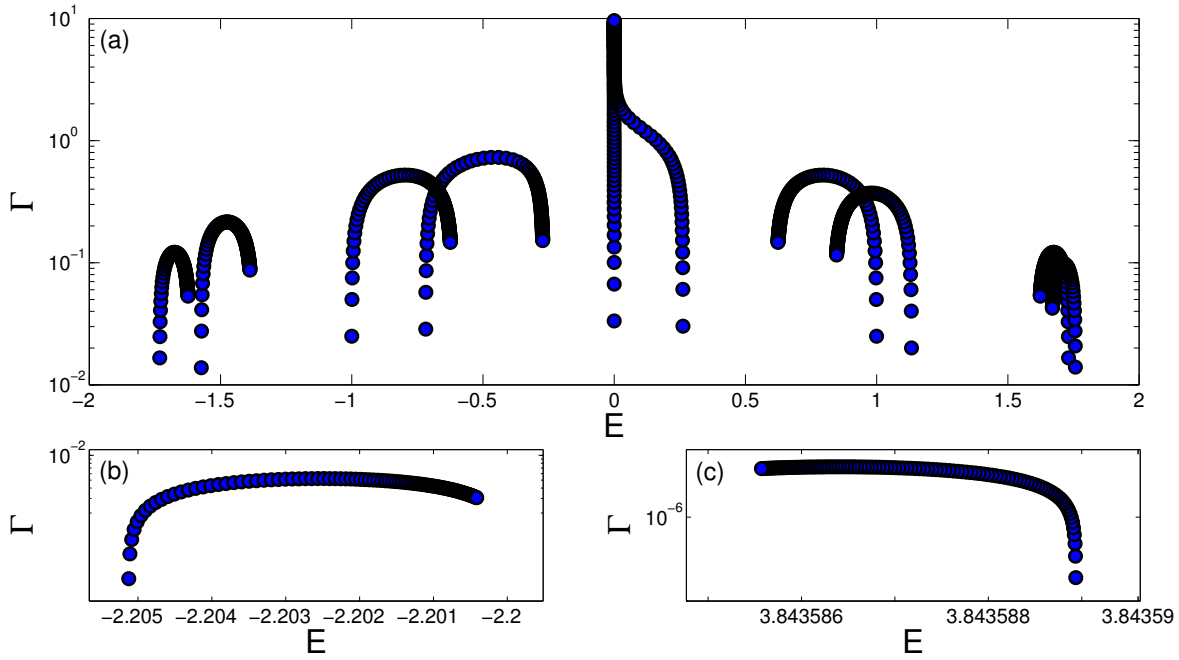

FIG. 6: (Color online). Complex-plane trajectories of eigenstates of the effective Hamiltonian; the parameters values are $v = 1,\ \lambda = 2.1,\ \Delta = 2.5$. Ten states, including the super-radiant at the edges of the chain, are moved closer inside the band, panel (a), two states mainly localized at the qubit have energies outside the band and essentially interact only with each other having a large lifetime with respect to tunneling through the chain, panels (b) and (c).

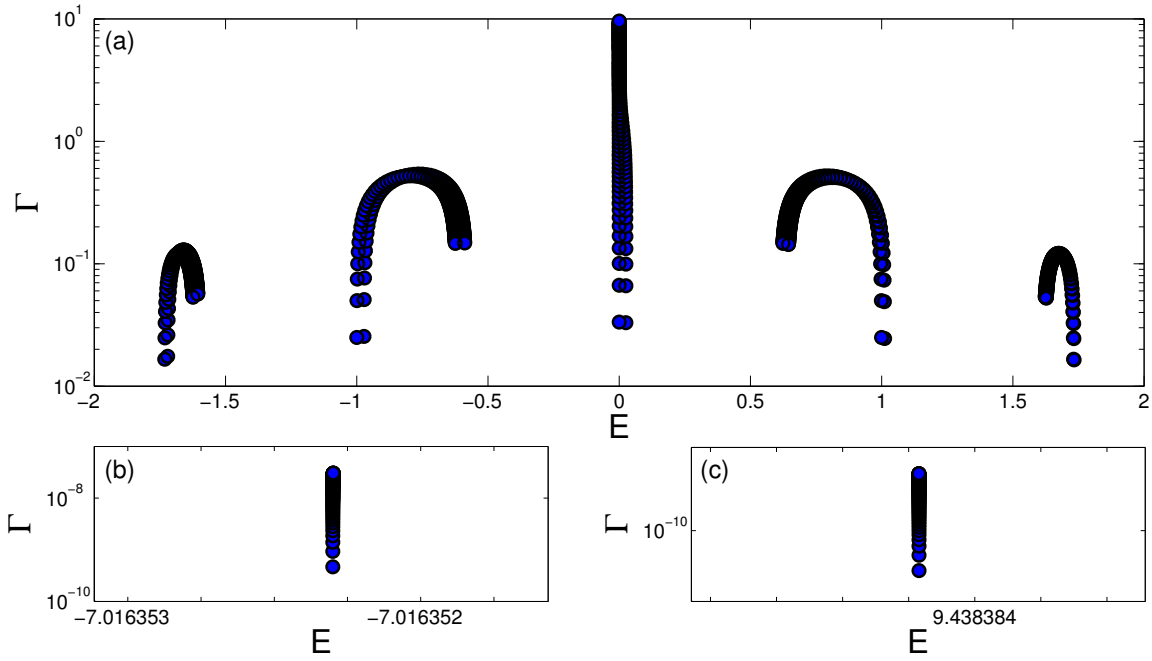

FIG. 7: (Color online). Complex-plane trajectories of eigenstates of the effective Hamiltonian; the parameters values are $v = 1,\ \lambda = 8,\ \Delta = 2.5$. Ten states, including the super-radiant at the edges of the chain, are moved closer inside the band, panel (a). The qubit states, the ground state, (b), and the excited state, (c), are essentially decoupled.

IV. TRANSMISSION THROUGH THE CHAIN

Here we briefly consider the transmission of an external signal through the chain with the inserted qubit, similarly to the consideration made earlier for the uniform chain or multi-dimensional lattices[12] and for the star graph[16]. The internal propagation of the signal of given energy E in the open system is described by the propagator

$$G(E) = \frac{1}{E - \mathcal{H}}, \tag{18}$$

where $\mathcal{H}$ is the effective Hamiltonian (15) with the imaginary part (16) that describes multiple excursions of the signal into continuum and back. Our simple geometry has two open channels, left and right (labeled L and R). The full amplitude Z^{ba} of the process between channels a and b starts with the entrance amplitude A_n^a that populates the intrinsic state $|n\rangle$ and ends with the exit amplitude A_m^{b*} from the intrinsic state $|m\rangle$; all paths $b \to a$ interfere:

$$Z^{ba}(E) = \sum_{mn} A_m^{b*} G_{mn}(E) A_n^a. \tag{19}$$

It is easy to show that the corresponding scattering matrix, $S^{ba} = \delta^{ba} - iZ^{ba}$, is unitary[3]. The transmission coefficient is given by

$$T^{ba}(E) = \left| Z^{ba}(E) \right|^2. \tag{20}$$

It might be convenient to perform the transformation to the (biorthogonal) basis $|r\rangle$ of eigenfunctions of the effective Hamiltonian. The complex energies $\mathcal{E}_r = E_r - (i/2)\Gamma_r$ correspond to the poles of the scattering matrix, while the process amplitude (19) still has factorized residues transformed to the eigenbasis,

$$Z^{ba}(E) = \sum_r \frac{\tilde{A}_r^b \tilde{A}_r^a}{E - \mathcal{E}_r}. \tag{21}$$

We can note parenthetically that this description can be treated as a simple superposition of interfering resonances only approximately, namely if the energy dependence of continuum amplitudes A_n^a is neglected as it is done in our consideration. In this approximation the time decay curve of a single isolated resonance $|r\rangle$ would be pure exponential with the width Γ_r.

For the calculation of transmission we adopt the approach of Ref.[12]. For the open chain of Sec. 3, the transmission is determined by the edge couplings which we again assume here to be equal, $\gamma_L = \gamma_R = \gamma$. Similarly to Ref.[12], the transmission coefficient (20) can be written as

$$T^{RL} = T^{LR} = \left| \frac{(\gamma/v^2)(E - \Delta)}{\prod_{r=1}^{2N+2} [(E - \mathcal{E}_r)/v]} \right|^2. \tag{22}$$

Below we show the transmission results for the chain of $N = 5$ (twelve intrinsic states) and various combinations of the parameters. The resulting picture is determined by the counterplay of the trend to super-radiation and decoupling of the qubit.

Starting with the weak qubit excitation amplitude, Fig. 8 for $\lambda = 0.1$, we follow the evolution of the transmission as a function of the continuum coupling γ. At small $\gamma = 0.1$, panel (a), we see twelve isolated resonances all having narrow decay widths; one of them is outside the energy band as we discussed earlier. When γ is growing, panels (b) and (c), the resonances start overlapping. When two super-radiant states merge at $\gamma = 2.4$, panel (c), they disappear from the transmission spectrum, so that panel (d) for $\gamma = 4$ shows ten separated resonances. At each resonance the transmission is perfect, $T = 1$.

Next four panels, Fig. 9, correspond to the intermediate value $\lambda = 2$. Again the case of weak continuum coupling, panel (a), $\gamma = 0.1$, reveals twelve resonances; now the two states associated with the qubit are outside the energy band, while all resonances still show perfect transmission. At $\gamma = \lambda = 2$, panel (b), the competition between the transmission through the chain and Rabi dynamics of the qubit leads to an almost random pattern of overlapping resonances with transmission below perfect, similar to Ericson fluctuations[15] or universal conductance fluctuations[27]. The relation between those well known pictures and necessary changes due to the effects of unitarity in exact theory were discussed in Ref.[11]. At large $\gamma \gg \lambda$, panels (c) and (d), the continuum coupling prevails leading to the narrow resonances coming from trapped intrinsic states.

Finally, the large value of the qubit excitation strength, $\lambda = 5$, changes the transmission picture at not very large γ, Fig. 10. At small continuum coupling, $\gamma \ll \lambda$, panel (a), the two states associated with the qubit produce two

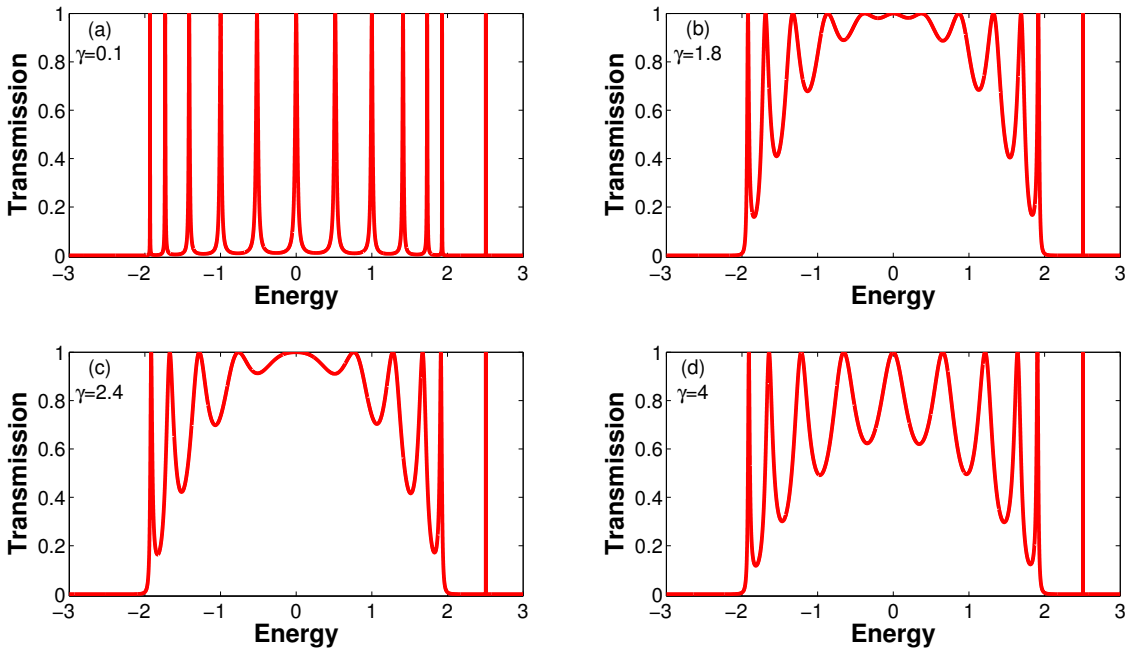

FIG. 8: (Color online). Evolution of the transmission for small $\lambda = 0.1$ as a function of the continuum coupling parameter $\gamma_L = \gamma_R = \gamma$, from 12 isolated resonances (one outside the energy band) through overlap and super-radiance to ten resonances corresponding to trapped states. As earlier, $\Delta = 2.5,\ v = 1$.

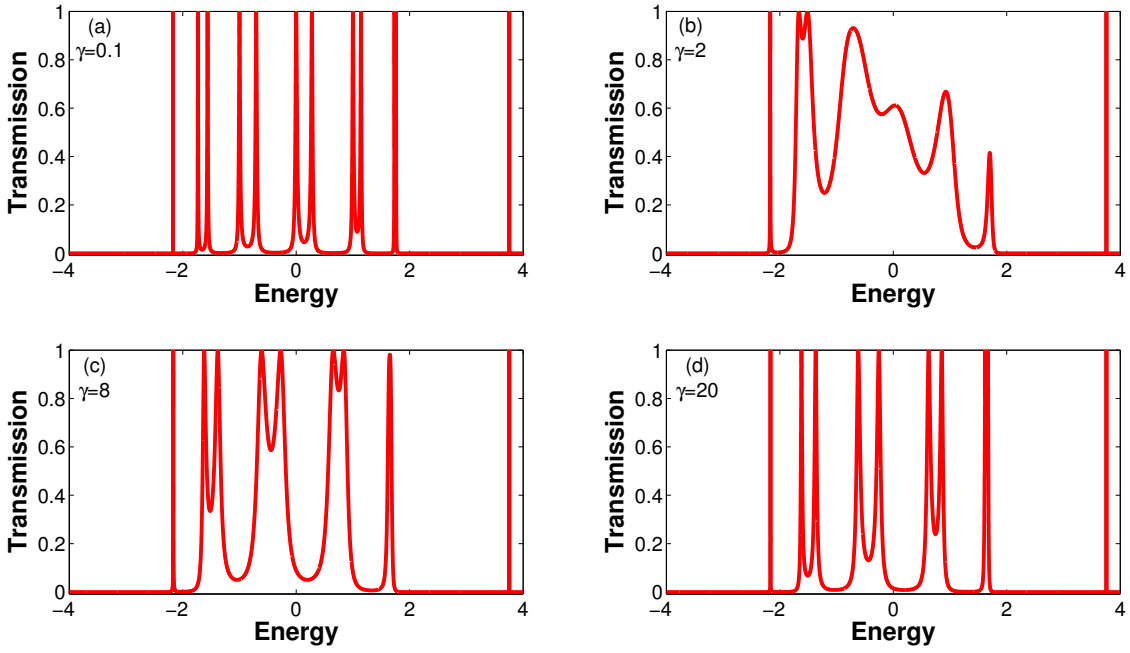

FIG. 9: (Color online). The same as Fig. 8, with $\lambda = 2$.

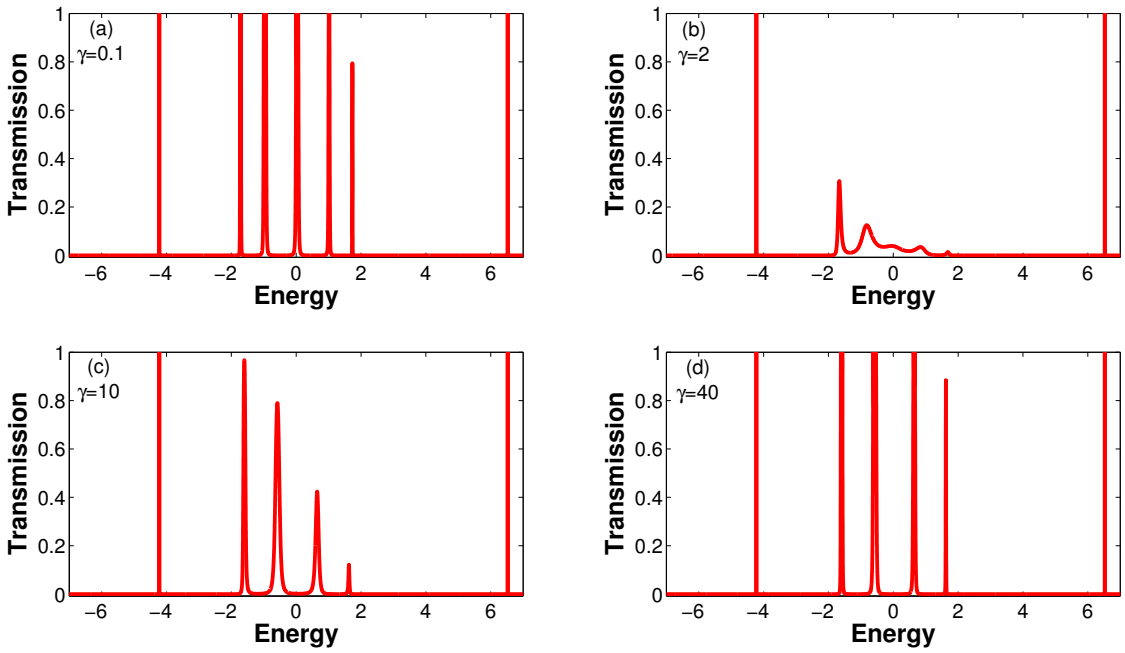

FIG. 10: (Color online). The same as Fig. 8, with $\lambda = 5$.

resonances outside the band, with transmission equal to 1. At $\gamma = 2$, panel (b), we observe some kind of an intrinsic resonance between propagation and internal oscillations which, along with the emergence of super-radiance, almost kills the transmission at other energies within the band. With further growth of γ, panels (c) and (d), the perfect transmission through trapped states, including those associated with the qubit, is gradually restored. This abundance of possible regimes opens the way to various applications.

V. CONCLUSION

Using the formalism of the effective non-Hermitian Hamiltonian, we studied a model of quantum signal transmission through a linear periodic chain with a qubit placed at the center. For the closed chain, the intrinsic eigenstates form two classes, antisymmetric standing waves with the excluded center site and two independent subchains, and symmetric that includes the qubit dynamics with two additional eigenstates. When the system is coupled to the environment, we have found the spectrum of quasistationary states characterized by complex energies and finite lifetimes. Two of those states are genetically related to the ground and excited state of the qubit with real energy outside the Bloch band.

The most interesting feature is the stability of states related to the qubit, small decay widths and correspondingly long lifetimes. Further, these states are only weakly perturbed when the coupling of the chain to the continuum becomes strong. In the limit of strong coupling, the qubit states and remaining trapped Bloch states are practically shielded from the external world by the two super-radiant states localized at the edges of the chain. The stability of the qubit states and the possibility to switch on and off the access to them suggests that the simple configuration considered above may serve as a building block of a quantum computer.

We discussed also the transmission through the chain as a function of the coupling strength to the continuum. In the limits of weak and strong continuum coupling (as compared to the excitation amplitude of the qubit) the chain reveals well separated narrow resonances with perfect transmission at corresponding energy. In the intermediate regime, when the continuum coupling and the excitation strength of the qubit are comparable, the resonances overlap with the transmission below the perfect level.

There are many possibilities to enrich this prototypical model. For a realistic situation, for example a chain of quantum dots, one should carefully determine the lifetimes of the qubit states. The geometry of the system can be made more complicated in various ways including the transition to more-dimensional schemes. More qubits and more

branches can be added approaching a complicated network. It would be also interesting to extend the ideology of an open quantum system to the study of coherent photon transport in circuit quantum electrodynamics[4,28,29].

VI. ACKNOWLEDGEMENTS

Y.G. acknowledges useful discussions with A.A. Shtygashev and partial support from the Russian Ministry of Education and Science through the project TP 7.1667.2011 and from the German Ministry of Science (BMBF) through the project RUS 10/015. C.M. is grateful for support at MSU in the framework of the REU program. V.Z. acknowledges the support from the NSF grant PHY-1068217.

[1] H. Feshbach, Ann. Phys. (N.Y.) **5**, 357 (1958); **19**, 287 (1962).
[2] C. Mahaux and H.A. Weidenmüeller, *Shell Model Approach to Nuclear Reactions* (North Holland, Amsterdam, 1969).
[3] N. Auerbach and V. Zelevinsky, Rep. Prog. Phys. **74**, 106301 (2011).
[4] S. Zhang, Z. Ye, Y. Wang, Y. Park, G. Bartal, M. Mrejen, X. Yin, and X. Zhang, Phys. Rev. Lett. **109**, 193902 (2012).
[5] G.L. Celardo, F. Borgonovi, M. Merkli, V.I. Tsifrinovich and G.P. Berman, cond-mat/1111.5443v1.
[6] R.H. Dicke, Phys. Rev. **93**, 99 (1954).
[7] *Super-radiance: Multiatomic Coherent Emission*, ed. M.G. Benedict (Taylor and Francis, N.Y., 1996).
[8] V.V. Sokolov and V.G. Zelevinsky, Ann. Phys. (N.Y.) **216**, 323 (1992).
[9] A. Volya and V. Zelevinsky, Journal of Optics B: Quantum and Semiclassical Optics, **5**, 450 (2003).
[10] A. Volya and V. Zelevinsky, Conf. Proc. **777**, *Nuclei and Mesoscopic Physics: WNMP 2004*, ed. by V. Zelevinsky (AIP, Melville, 2005) p. 229.
[11] S. Sorathia, F.M. Izrailev, G.L. Celardo, V.G. Zelevinsky, and G.P. Berman, EPL **88**, 27003 (2009).
[12] G.L. Celardo, A.M. Smith, S. Sorathia, V.G. Zelevinsky, R.A. Sen'kov, and L. Kaplan, Phys. Rev. B **82**, 165437 (2010).
[13] S. Sorathia, F. M. Izrailev, V. G. Zelevinsky, and G. L. Celardo, Phys. Rev. E **86**, 011142 (2012).
[14] G.L. Celardo and L. Kaplan, Phys. Rev. B **79**, 155108 (2009).
[15] T. Ericson, Ann. Phys. (N.Y.) **23**, 390 (1963).
[16] A. Ziletti, F. Borgonovi, G.L. Celardo, F.M. Izrailev, L. Kaplan, and V.G. Zelevinsky, Phys. Rev. B **85**, 052201 (2012).
[17] Zh. Tang and N.A. Kotov, Adv. Mater. **17**, 951 (2005).
[18] S. Longhi, Phys. Rev. Lett. **97**, 110402 (2006).
[19] H. Nakamura, N. Hatano, S. Garmon, and T. Petrosky, Phys. Rev. Lett. **99**, 210404 (2007).
[20] A.D. Dente, R.A. Bustos-Marun, and H.M. Pastawski, Phys. Rev. A **78**, 062116 (2008).
[21] S. Garmon, T. Petrosky, L. Simine, and D. Segal, Fortschr. Phys. **61 issue 2-3** (2013).
[22] L. Durand, Phys. Rev. D **14**, 3174 (1976).
[23] N. Auerbach and V. Zelevinsky, Nucl. Phys. **A781** (2007) 67.
[24] G. Shchedrin and V. Zelevinsky, Phys. Rev. C **86**, 044602 (2012).
[25] K. Sasada and N. Hatano, Physika E **29**, 609 (2005); K. Sasada, N. Hatano, and G. Ordonez, arXiv:0905.3953.
[26] P. von Brentano, Phys. Rep. **264**, 57 (1996).
[27] C.W.J. Beenakker, Rev. Mod. Phys. **69**, 731 (1997).
[28] J.-Q. Liao, Z.R. Gong, L. Zhou, Y.-X. Liu, C.P. Sun, and F. Nori, Phys. Rev. A **81**, 042304 (2010).
[29] M. Delanty, S. Rebic, and J. Twamley, New J. Phys. **13**, 053032 (2011).